Proceedings of ISFOG 2025
5TH INTERNATIONAL SYMPOSIUM ON
FRONTIERS IN OFFSHORE GEOTECHNICS
Nantes, France | June 9-13 2025

ISBN 978-2-85782-758-0

Feasibility of using driven monopiles in weak rock to support offshore wind turbines

S. Maclean I. A. Richards*, G. Pittos, P. Knight
Wood Thilsted, London, UK

iar@woodthilsted.com (corresponding author)

ABSTRACT: As the offshore wind industry continues to grow its global footprint, an increasing number of offshore wind farms are being developed at sites with bedrock within the foundation depth. Where these sites have sufficiently shallow water depths and where the bedrock is weak or weathered and sufficiently deep, a driven monopile may be the preferred foundation solution. In these conditions, the rock will reduce the required monopile length but also increase the driving refusal risk. For an example site consisting of high-strength clay over weak rock, this paper explores the impact of rock properties and confidence in rock characterisation on monopile design and driveability, and therefore foundation feasibility. With relatively limited industry experience designing and installing driven piles in weak rock, this paper also compares available methods for driveability prediction and proposes a formulation for the base (S-y) reaction in rock.

Keywords: Monopiles; rock; driveability; offshore wind

1 INTRODUCTION

Driven monopile foundations are widely used to support offshore wind turbines. These large-diameter, thin-walled piles are structurally efficient and have an established supply chain, hence, they are generally the preferred foundation solution at sites with sufficiently shallow water depths and driveable soil conditions. As the offshore wind industry grows its global footprint, an increasing number of offshore wind farms are being developed at sites with bedrock within the foundation depth. Where the bedrock is sufficiently weak or weathered, it is possible to install monopiles some meters into the bedrock by impact driving, making a driven monopile solution feasible and likely economically preferred. This paper explores the impact of rock properties and the confidence in rock characterisation on the feasibility of a driven monopile solution for an example site.

2 METHODOLOGY

2.1 Site conditions

The example site has 30 m water depth, with the stratigraphy consisting of 25 m of high-strength clay overlying mudstone. The applied clay properties, which vary linearly with depth, are shown in Table 1. Note that a conservative value for CPT cone resistance is taken for input to driveability assessment, to account for uncertainties, although as driveability is governed by the rock this has negligible impact on the results.

The mudstone properties are varied to explore the impact on monopile feasibility. Unconfined Compressive Strength, UCS, for intact rock and Rock Quality Designation, RQD, together capture rock strength and quality and are used as the primary variables in this study. Applied UCS values range from 1 MPa to 35 MPa in increments of 5 MPa. For each UCS increment, values of RQD range from 20% to 100% in increments of 20%. Other parameters required for design and driveability assessment (Young's Modulus, E, small strain shear modulus, G_0, and Geological Strength Index, GSI) are derived from UCS and RQD based on existing correlations.

In rock mechanics, it is important to distinguish between, and characterise, both the intact material, i, and the in-situ discontinuous rock mass, m. Whether intact or rock mass properties are relevant depends on the scale and mechanism associated with the geotechnical analysis performed, relative to the scale of rock mass features.

Table 1. Properties for clay: effective unit weight, γ'; undrained shear strength, c_u; small strain shear modulus, G_0; corrected cone resistance, q_t; sleeve friction, f_s.

Depth (m)	γ' (kN/m³)	c_u (kPa)	G_0 (MPa)	q_t (MPa)	f_s (kPa)
0	10	80	25	5	50
25	10	120	50	5	50

Young's Modulus for intact rock, E_i, can be considered a function of UCS using the Modulus Ratio, MR (Deere, 1968). In this study, an MR of 1300 is assumed based on Look et al. (2016). To determine Young's Modulus for rock mass, E_m, the correlation from Zhang and Einstein (2004) is applied:

$$E_m = E_i 10^{0.0186RQD-1.91} \tag{1}$$

GSI is troublesome to define for offshore purposes given that traditionally outcrop-scale descriptions are needed. Taking a simplified approach, here GSI is considered a function of RQD through the assumption of a Joint Condition, J_{cond89} (Bieniawski, 1989), where J_{cond89} is taken as 20. For derivation of $G_{0,i}$ and $G_{0,m}$ from E_i and E_m respectively, a Poisson's ratio of 0.2 is assumed. Lastly, UCS_m is determined from intact strength using adjustment factor, j, which is a function of RQD (Gannon et al., 1999):

$$UCS_m = j\, UCS \tag{2}$$

For simplicity, all rock properties are constant with depth. Beside the rock properties, the rock elevation and clay properties also play a crucial role in monopile feasibility. While these aspects are not explored quantitatively, they are discussed in Section 3.

2.2 Monopile design

Monopile design is performed using a 1D analysis model with the pile represented by Timoshenko beam elements. The geotechnical-structure interaction is described by non-linear reaction curves. For these analyses, distributed lateral (*p-y*) and base lateral (*S-y*) curves are applied, as described in Section 2.3. The monopile embedment depth is determined such that the monopile has sufficient over-turning capacity to resist the ultimate limit state design loads. Table 2 presents the design overturning moment, M, and shear force, Q, applied at seafloor, which are representative for a 15 MW turbine under mild to moderate metocean conditions. For practical design, monopile embedment may be determined by serviceability limit state requirements or clustering requirements, however, this ultimate limit state criteria provides a reasonable basis for this feasibility assessment. The monopile diameter, D, and wall thickness at the pile base, t_B, are also presented in Table 2.

Table 2. Design overturning loads at seafloor (inclusive of partial load factors) and fixed monopile dimensions.

M (MNm)	Q (MN)	D (m)	t_B (m)
650	10	10	0.11

2.3 Geotechnical reaction curves

The clay is modelled with *p-y* and *S-y* curves according to the PISA rule-based formulations (Byrne et al., 2020). For practical design, site-specific calibration of the soil reaction curves to 3D finite element (FE) analyses is required, alongside a detailed cyclic degradation assessment.

The mudstone is modelled with *p-y* curves based on the formulation presented by Reese (1997). However, the original publication is unclear on whether the input strength parameter should be representative of intact rock or a rock mass. Moreover, the formulation includes a strength reduction factor, α_r, which is a function of RQD such that in highly fractured rock masses the *p-y* capacity will be higher than for an intact rock mass, when an intact strength parameter is applied. This is based on onshore observations of shallow failure modes and is not seen as applicable to many offshore scenarios due to significant overburden soil. Hence, in this work, α_r is taken as unity and UCS_m is applied as the strength parameter. In the formulation presented by Reese (1997), displacement parameter, k_{rm}, is also an important parameter for monopile design, controlling the intermediate stiffness of the *p-y* curve. Reese suggests a value between 0.0005 and 0.00005; in this work, an intermediate value (0.000275) is applied.

No established *S-y* reaction curve for monopiles in rock exists, however, for a driven pile, the base reaction is expected to make a significant contribution to the overturning capacity. Hence, for application in this work, a simplified base reaction curve for driven piles in weak rock is derived from first principles, considering that displacement at the pile base will involve shearing the surrounding rock mass. The *S-y* capacity is determined as:

$$S_u = A_{base} \frac{UCS_m}{2} \tag{3}$$

Where A_{base} is the (enclosed) pile base area. The displacement of the *S-y* curve is determined based on the shear stiffness modulus definition of the rock mass, G_m:

$$G_m = \frac{\tau}{\gamma} = \left(\frac{S}{A_{base}}\right)\left(\frac{y}{l}\right)^{-1} = \frac{Sl}{yA_{base}} \tag{4}$$

$$y = \frac{Sl}{G_m A_{base}} \tag{5}$$

Where l is the thickness of the mobilised rock mass, assumed to be equal to the pile diameter, D. Here, the *S-y* reaction curve is modelled with a constant stiffness derived from the small strain shear modulus for rock mass, $G_{0,m}$, as shown in Figure 1.

While this design approach for rock is considered rational and suitable for feasibility assessment, the experimental database on which design methods for driven piles in rock can be derived is very limited. Indeed, Reese (1997) presents their *p-y* curves as "interim" due to the meagre amount for experimental data available, and the publicly available database has not grown significantly in the intervening period. For detailed design, validation of the presented methods against pile load tests, in combination with advanced 3D finite element analyses, is recommended, and will likely reduce the pile dimensions and hence increase the feasibility.

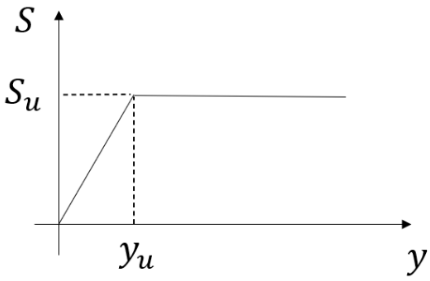

Figure 1. S-y reaction curve derived from first principles.

2.4 Driveability assessment

Driveability assessment is performed using a 1D wave equation analysis model, with the geotechnical-structure interaction modelled using resistance to driving curves described in Section 2.5. A hammer with maximum operating impact energy 5500 kJ, 2.0 m stroke height and 95% efficiency is applied. Refusal is determined when more than 1000 blows per meter are required over a driving analysis depth of 0.2 m. No relief drilling is considered as part of this assessment, *i.e.* no reduction of internal shaft friction or base resistance is applied.

2.5 Resistance to driving

For clay, the established CPT-based method presented by Maynard et al. (2019) is used to model the resistance to driving. Pile driving in rock is much less common than pile driving in clay and sand. Hence, the databases on which resistance to driving formulations can be based are limited, and no widely accepted or applicable method for predicting driving in rock exists. Table 3 summarises some of the available methods based on back-analysis of driving logs (Stevens et al., 1982; Kadiver et al., 2024) and a method based on back-analysis of pile load tests (Terente et al., 2017) which can be tentatively applied for driveability prediction. This list is not exhaustive, and does not include methods based on CPT measurements, such as presented by Jones et al. (2020), nor other methods based on back analyses of pile loads tests, e.g. by Zhang & Einstein (1998). In this work, two methods are used, one combining the works of Stevens et al. (1982) and Terente et al. (2017), and the other applying the more recent approach given by Kadiver et al. (2024), as summarised in Table 4.

Table 4. Driveability methods applied.

Method	*Q-z*	*t-z*
S-T	Stevens et al. (1982)	Terente et al. (2017)
Kadiver	Kadiver et al. (2024)	Kadiver et al. (2024)

The details of the applied driveability methods are outlined in Table 3 and Table 5. A key difference between the two approaches used is the Terente t-z methodology, used alongside Stevens Q-z, considers rock mass strength and takes RQD as an input. Conversely, the Kadiver approach uses intact strength values, not accounting for rock mass behaviour directly.

Table 3. Methods for modelling driveability in weak rock (Q-z).

Stevens et al. (1982)	• This widely applied method is based on driving back-analysis for a small number of piles installed through layers of poor-quality sandstone and gypsum. • Base resistance is proportional to UCS with bearing factor $N_u = 3$, and is limited to values given by Stevens et al. (1982) for granular soils. Stevens states that driveability evaluation should be based on RQD, however, this method does not account for rock quality.
Kadiver et al. (2024)	• This method presents an advancement of the method from Stevens et al. (1982) based on driving back-analysis for monopiles installed into very weak to weak Mercia Mudstone. • Base resistance is proportional to intact UCS with bearing factor $N_u = 5$.

Table 5. Methods for modelling driveability in weak rock (t-z).

Stevens et al. (1982)	• This method assumes that driving reduces the rock to a granular material, hence, shaft resistance is a function of a representative interface friction angle, δ.
Kadiver et al. (2024)	• Shaft resistance is a function of UCS only, with a cap on shaft resistance of 1 MPa.
Terente et al. (2017)	• This method is based on ~20 pile load tests of driven piles in weak rock (siltstones, sandstones and limestone). • Shaft capacity is a function of rock mass strength UCS_m and adhesion factor, α, which is itself a function of UCS_m. For application for driveability, a more cautious expression for α is applied ($\alpha = 0.25UCS_m^{-0.5}$).

3 FEASIBILITY RESULTS

3.1 Impact of rock properties

Figure 2 presents required pile embedment into bedrock for the example site, applying the methods described in Section 2.2 and 2.3, and varying UCS and RQD. As expected, required pile embedment reduces both with increasing UCS and increasing RQD. Strength has a greater influence on the embedment than rock mass quality, although for UCS > 5 MPa neither parameter significantly influences the rock embedment. For RQD = 0.2, varying UCS from 1 MPa to 30 MPa results in embedment from ~20 m into bedrock to <3 m, highlighting the major impact of rock strength on design. Additionally, for UCS of 1 MPa, varying RQD from 0.2 to 1 result in rock embedment reducing from ~20 m to ~6 m. It is acknowledged here that pile designs presented for the most extreme cases are unrealistic, with lengths approaching 100 m. However, this is an exercise to investigate purely the impacts of rock parameters on conceptual feasibility and does not explore realities of manufacturing and transportation, and as such values are seen appropriate.

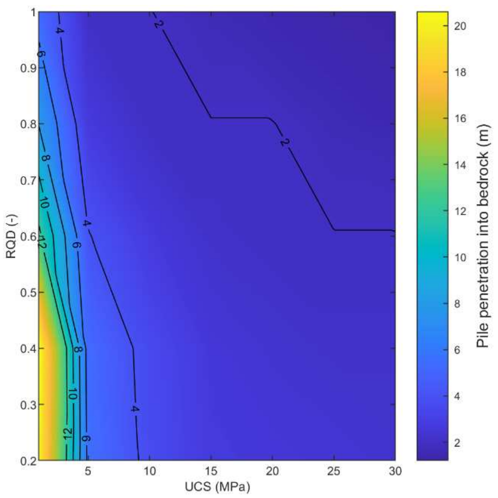

Figure 2. Pile embedment into bedrock for various UCS and RQD.

Driveability results, applying the methods described in Section 2.4 and 2.5, are presented in Figure 3 and Figure 4, for the Stevens-Terente (S-T) and Kadiver methods, respectively. Both methods predict earlier refusal with increasing UCS, however, the Kadiver method predicts far shallower refusal, with maximum 5 m driving embedment into bedrock, compared with S-T predicting up to 20 m bedrock penetration for poor-quality, low-strength rock. The influence of RQD in the S-T results is apparent with greater refusal depths predicted at low RQD, although at sufficiently high UCS the influence of RQD becomes less apparent, and beyond 25 MPa both methods show similar results with very shallow refusal. Given the fairly limited databases on which these driveability methods are derived, it is considered that both the S-T and Kadiver methods present plausible driveability results. It is noted that the Kadiver Q-z is based on the Stevens approach but instead uses a bearing capacity factor of 5 compared to the original 3 (Stevens et al., 1982). Should the Stevens approach used here be updated to apply a higher bearing factor, the results would be more similar.

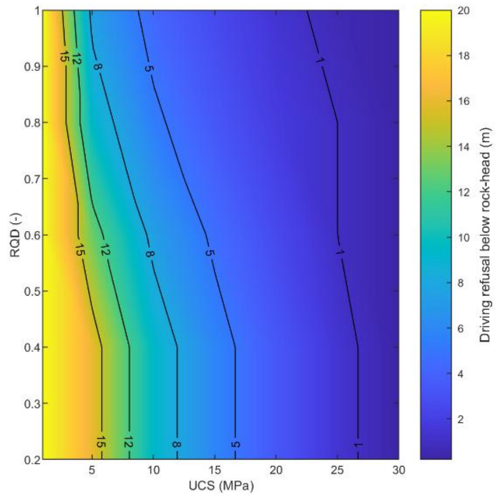

Figure 3. Driving refusal depth below rock-head when using the S-T driveability approach.

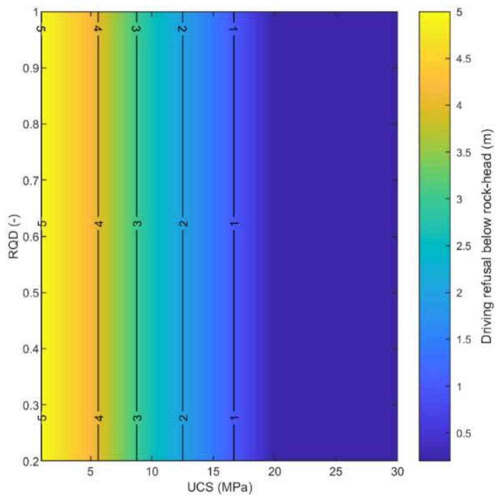

Figure 4. Driving refusal depth below rock-head when using the Kadiver driveability approach.

By combining the design pile embedment with the driving refusal predictions, it is possible to estimate feasibility of driven monopiles at this example site. The results are shown in Figure 5 for the Kadiver and S-T driveability methods. It is apparent that these methods show significantly different feasibility predictions, with the Kadiver approach giving a far more limited prediction of feasibility. The S-T method shows a driven monopile solution is feasible for $UCS \leq 20$ MPa whilst Kadiver demonstrates feasibility only at half that strength or less. Kadiver, lacking any consideration for RQD, shows feasibility only for UCS of 5–10 MPa and at high RQD, where design pile lengths are shorter. In contrast, the S-T method accounts for RQD in the driveability predictions, and as such shows that pile installation is feasible for all RQD levels for UCS 5–15 MPa and for $RQD > 0.6$ for UCS 1 MPa, and < 0.6 for UCS 20 MPa. Neither method predict that a driven monopile is feasible in very poor quality weak rock, nor in stronger rock of UCS >20 MPa.

These results highlight the importance of the selected design and driveability methods for determining foundation feasibility, and the challenge in determining feasibility where there is uncertainty in the applied methods. They also highlight the importance of proper rock-mass characterisation in rock engineering and the need for future driveability back-analysis that accounts for fracturing.

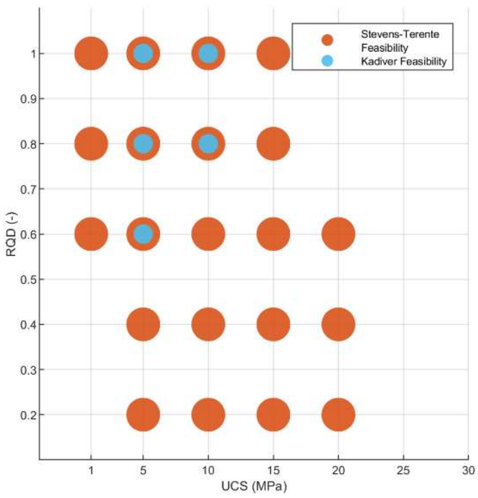

Figure 5. Monopile feasibility for various UCS and RQD.

3.2 Impact of uncertainty in rock characterisation

In practice, there always remains inherent uncertainty in the geotechnical parameters to apply for design at a given location, due to spatial variability in properties and testing limitations. Typically, cautious (B) and optimistic (D) best estimate parameter bounds are defined, to account for this. Such bounds are usually based on a statistical relationship where D often represents the mean plus some percentage of the standard deviation and B the mean minus some percentage of the standard deviation. Typically, design is determined using B parameters and driveability is determined using D parameters, such that geotechnical conditions are cautiously assumed to be weaker for design and stronger in driveability (DNV, 2021).

To illustrate the impact of applying different parameter bounds for design and driveability here, feasibility is re-assessed with pile embedment based on lower UCS relative to driveability (for the same RQD). The UCS values applied for driveability being UCS plus 5 MPa higher than those used for the equivalent design. Using this approach, the range where a driven monopile is feasible reduces to those shown in Figure 6.

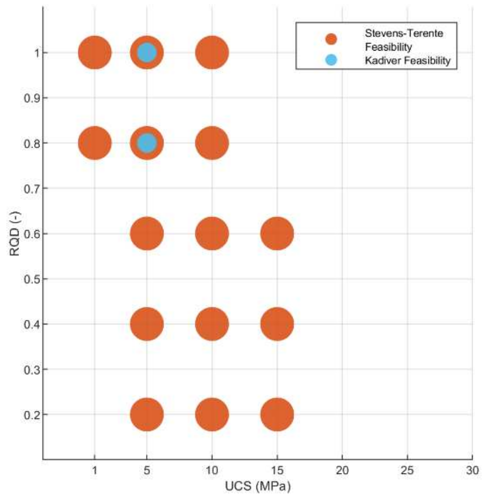

Figure 6. Monopile feasibility for various UCS and RQD, where uncertainty in rock characterisation is considered.

These results show further limited feasibility of driven monopiles in rock. Feasibility with the S-T method is reduced to a maximum UCS of 15 MPa, with Kadiver now only showing feasibility at UCS of 5 MPa. This highlights the significant impact of confidence in geotechnical characterisation feasibility. Where sufficient, potentially position-specific, data is available and there is high confidence in the geotechnical parameters, feasibility will increase. However, such confidence is often not available for early-stage assessments, challenging this kind of work.

3.3 Feasibility at other sites

In this work, the rock is assumed homogenous with depth. However, in practice, a variation in depth is likely with an upper weathered zone and increasing rock mass quality with depth. For such sites, the rate of increase in rock strength and stiffness will be key in determining feasibility. This work also applies a constant rockhead elevation of 25 m below seafloor. This elevation will have significant impact on feasibility for driven monopiles, and it can be expected that a shallow rockhead will limit feasibility. Lastly, a simple high-strength clay is assumed in this work, however, it is clear that any overlying soil will also impact the feasibility for driven monopiles. Where soil has significant capacity to limit embedment into rock, the feasibility of such a solution will increase, hence, characterisation of the overlying soils is also crucial.

4 CONCLUSIONS

This paper has explored the feasibility of driven monopiles in weak rock for an example site, where high-strength clay overlies mudstone at 25 m below seafloor. The results show that feasibility varies significantly with the selected driveability method, highlighting the importance of selecting suitable methods, ideally based on robust back-analysis in similar geotechnical conditions, for such feasibility assessments. However, where there is uncertainty on the most suitable methods to apply, understanding the impact of the selected methods, as explored in this paper for driveability, is crucial. This paper also illustrates the impact of the confidence in rock characterisation on feasibility. Where there is low confidence in the rock characterisation, feasibility significantly reduces, as cautious parameters are applied for design and cautious parameters for driveability. This demonstrates the value in obtaining sufficient high-quality geotechnical data at early-stage, to inform such feasibility assessments.

5 AUTHOR CONTRIBUTION STATEMENT

S. Maclean: Conceptualisation, Methodology, Formal Analysis, Writing – Original Draft.

I. A. Richards: Methodology, Writing – Review & Editing, Reviewing, Supervision.

G. Pittos: Reviewing – Review & Editing.

P. Knight: Reviewing – Review & Editing.

REFERENCES

Barrett, J.W. and Prendergast, L.J. (2020). Empirical Shaft Resistance of Driven Piles Penetrating Weak Rock, *Rock Mechanics and Rock Engineering*, 53.

Bieniawski, Z. T. (1989). Engineering rock mass classifications : a complete manual for engineers and geologists in mining, civil, and petroleum engineering. Wiley-Interscience.

Byrne, B.W., Houlsby, G.T., Burd, H.J., Gavin, K.G., Igoe, D.J.P., Jardine, R.J., Martin, C.M., McAdam, R.A, Potts, D.M., Taborda, D.M.G. and Zdravković, L. (2020). PISA design model for monopiles for offshore wind turbines: application to a stiff glacial clay till, *Géotechnique*, 70(11).

DNV, 2021. *DNV-RP-C207 Statistical representation of soil data*. Recommended Practice. Edition 2019-09, amended 2021-09. DNV.

Gannon, J.A., Masterton, G.G.T, Wallace, W.A. and Muir Wood D. (1999). Piled Foundations in Weak Rock, CIRIA. Report 181.

Clausen, J. (2013). Bearing capacity of circular footings on a Hoek-Brown material, *International Journal of Rock Mechanics and Mining Sciences,* 57.

Deere, D.U. (1968). Chapter 1: Geological considerations, In: *Rock Mechanics in Engineering Practice*. London: John Wiley and Sons.

Jones, L., Rattley, M., Manceau, S. (2020). A CPT-based soil resistance to driving (SRD) method for offshore pile driveability analyses, In: *Piling 2020*.

Kadiver, M., Ghasemi, P., Christopher, N., Maynard, A., and Barwise, A. (2024). Pile Driveability Through Rock Formations, In: *Offshore Technology Conference*, Houston, Texas.

Look, B., Schneider, S. & Gallage, C. (2016). Characterisation of Small Strain Rock Modulus from Ultrasonic Pulse Velocity Testing. In: *Geotechnical and Geophysical Site Characterisation 5*. Australian Geomechanics Society, Sydney, Australia.

Maynard, A.W., Hamre, L., Butterworth, D., and Davison, F. (2019). Improved Pile Installation Predictions for Monopiles, In: *10th International Conference on Stress Wave Theory and Testing Methods for Deep Foundations*.

Reese, L.C. (1997). Analysis of Laterally Loaded Piles in Weak Rock, *Journal of Geotechnical and Geoenvironmental Engineering*, 123(11).

Stevens, R.S., Wiltsie, E.A., and Turton, T.H. (1982). Evaluating Pile Driveability for Hard Clay, Very Dense Sand, and Rock, In: *14th Annual Offshore Technology Conference,* Houston, Texas.

Terente, V, Irvine, J., Torres, I., Jaeck, C. (2017). Driven Pile Design Methods in Weak Rock. In: *8th International Conference Offshore Site Investigation and Geotechnics*, London, UK.

Zhang, L., and Einstein, H.H. (1998). End Bearing Capacity of Drilled Shafts in Rock, *Journal of Geotechnical and Geoenvironmental Engineering*, 124(7).

Zhang, L., & Einstein, H.H. (2004). Using RQD to estimate the deformation modulus of rock masses, *International Journal of Rock Mechanics and Mining Sciences*, 41.